JOURNAL OF MATERIALS SCIENCE 23 (1988) 761–768

Physical and mechanical properties of $YBa_2Cu_3O_{7-\delta}$ superconductors

N. McN. ALFORD, J. D. BIRCHALL, W. J. CLEGG, M. A. HARMER, K. KENDALL
ICI Advanced Materials, PO Box 11, The Heath, Runcorn, WA7 4QE, UK

D. H. JONES
Physics Department, Liverpool University, PO Box 147, Liverpool L69 3BX, UK

The physical and mechanical properties of $YBa_2Cu_3O_{7-\delta}$ superconductors are examined. These properties are related to powder preparation method, powder characteristics, sintering behaviour and sintered microstructure. The sintering atmosphere and sintering schedules affect the final microstructure very strongly and determine, in conjunction with starting powder characteristics, the sintered density. The mechanical properties such as Young's modulus, bend strength and critical stress intensity factor (fracture toughness) are measured and related to microstructure as determined by electron microscopy. Control of microstructure by careful powder selection and sintering schedule is seen as key to optimizing the physical and mechanical properties of the material. Finally attention is drawn to fabrication techniques and how these must be optimized in order to realize the mechanical properties which are necessary if these are to be useful as engineering materials. Comparisons between fabrication techniques show that uniaxial powder pressing suffers from limitations in terms of specimen complexity and densification whereas the favoured route, termed viscous processing, gives a more homogeneous microstructure, higher strength and allows near theoretical density to be achieved.

1. Introduction

The discovery of superconductivity in the region 30 K by Bednorz and Muller [1, 2] in the La–Ba–Cu–O system generated enormous interest. Substitution of La by Y [3] indicated that superconductivity could exist in these ceramics above liquid nitrogen temperatures.

In this paper we deal with the $YBa_2Cu_3O_{7-\delta}$ system concentrating attention on the fabrication and the physical and mechanical properties of the materials. Hitherto much of the research has been devoted to the determination of phase by TEM and XRD of the various superconducting copper oxides [4, 5, 6, 7]. Oxygen stoichiometry is clearly of key importance in determining the T_c, where T_c is the superconducting transition temperature, and the width of the transition and much work has been carried out in this area [8, 9].

If these materials are to find practical uses then their mechanical properties must be known. It is generally stated that these materials are brittle but so is silica fibre which has a tensile strength of several GPa and can be twisted round a finger.

There is a need to quantify the mechanical and physical properties such as toughness, strength, Young's modulus, porosity and density in order to make sensible judgements on the practical usage of the materials and to define their limitations. In this paper we examine the physical and mechanical properties of the $YBa_2Cu_3O_{7-\delta}$ superconductors and relate both the superconducting and physico-mechanical properties to the microstructure as determined by SEM and optical microscopy.

2. Experimental Procedures

2.1. Powder preparation

Y_2O_3 (99.9% Rare Earth Products), $BaCO_3$ (Fluka 99.9%) and CuO (Fluka 99.9%) were mixed in a high energy vibro mill with ZrO_2 media in ethanol. The slurry was dried using a rotary evaporator and then the powder was calcined in air at 950° C for 12 h. The sintered fragments were then vibro milled in ethanol for 72 h and dried in the same manner. The surface area of this powder was $5.9\,m^2\,g^{-1}$.

2.2. Sample preparation

Samples were prepared by two different methods.

(1) *Powder pressing*

The powders were uniaxially powder pressed into discs 10 mm or 25 mm in diameter. The green density of these discs was ~ 50% of theoretical.

(2) *Viscous processing*

The powder was also processed in a viscous medium according to the method described in [10]. This was achieved by mixing a viscous polymer solution with the powder. The solids fraction was ~ 0.52. This mixture was first processed on a two roll mill until a homogeneous mixture formed and then this mixture was extruded in a 13 mm ram extruder through a series of dies ranging from 0.2 to 4 mm in diameter to

0022–2461/88 $03.00 + .12

produce a series of cylindrical rods. The rods were dried at 80° C before firing.

The $YBa_2Cu_3O_{7-\delta}$ powder was found to be reactive if processed in aqueous media, therefore non aqueous solvents and polymers soluble in such solvents were used instead.

2.3. Sintering/Dilatometry

Sintering was carried out in a silica tube encased within an alumina tube furnace. The samples were placed on porous alumina plates. The atmosphere was flowing oxygen. Sintering temperatures varied between 850 and 980° C and various sintering times were used in order to vary density and grain growth. All samples were pressureless sintered.

Dilatometry was performed on a Netszch 402E (Selb, W. Germany) dilatometer in air or flowing oxygen within an alumina tube. Thermal coefficient of expansion was measured on sintered samples both in air and flowing oxygen.

2.4. Microstructural examination

The samples were examined by both light microscopy and electron microscopy. The samples were uncoated for the purposes of electron microscopy. Electron probe micro-analysis (EPMA) was used to determine compositional homogeneity within the samples. EPMA samples were ground and finally polished on 0.25 μm diamond paste.

2.5. T_c measurement, electrical resistivity, critical current

The samples were characterized by resistivity measurements using a flow cryostat. Critical current was measured at 77 K. The resistance was measured using an AC bridge and a sensing current of 1 mA or less. Under these conditions point contacts were found to give reproducible results.

2.6. Mechanical and physical properties

2.6.1. Density

Density was determined on fired discs or cylindrical rods by mass and dimensions. Porosity was determined by determining the ratio between the apparent density and the theoretical density which was calculated from lattice parameter data to be 6.38 g cm^{-3} [8].

2.6.2. Fracture toughness

The critical stress intensity factor K_{IC} was determined by single edge notched beam using Equation 1.

$$K_{IC} = \sigma_f Y \sqrt{c} \quad (1)$$

where σ_f is flexural strength of the notched beam, c is the notch depth and Y is a function relating to specimen geometry and loading configuration. Y is given in ref. [11] as

$$Y = 1.93 - 3.07(c/d) + 14.53(c/d)^2 - 25.11(c/d)^3 + 25.8(c/d)^4 \quad (2)$$

where d is beam depth. The beams were cut from plates of prefired material on a diamond saw. The dimensions of the beams were (approximately) length = 30 mm, width = 2 mm, depth = 5 mm. The notch was cut after firing using a slow speed diamond saw. The notch width was 0.2 mm.

2.6.3. Flexural strength

Flexural strength, σ_f, was determined on ~0.9 mm cylindrical rods over a span, L, of 20 mm using Equation 3

$$\sigma_f = 8PL/\pi D^3 \quad (3)$$

where P is load and D is rod diameter.

Young's modulus in bending, E_b, was measured on ~0.9 mm diameter rods using Equation 4

$$E_b = 4PL^3/3y\pi D^4 \quad (4)$$

where y is deflection at the mid point of the beam.

Strength and Young's modulus were determined on a 5KN Instron 1135 testing machine. Flexural strength was determined using a span of 20 mm and crosshead speed of 5 mm min^{-1}. Young's modulus was determined on a 30 mm span and a crosshead speed of 0.2 mm min^{-1}.

The rods for strength and modulus testing were viscous processed materials tested in the as fired condition. No machining of any sort was undertaken prior to testing.

2.7. Thermal conductivity and specific heat

Thermal diffusivity was measured by the heat pulse method. The pulse was delivered by a high power photographic flash tube and the time taken for the heat pulse to travel from the face to the back of the sample was measured. The temperature was recorded by means of a thermocouple.

Specific heat was measured using a Perkin Elmer DSC 7 differential scanning calorimeter calibrated against a sapphire standard. The experiment was conducted at 24° C.

3. Results and Discussion

3.1. Densification of material depended on a series of factors including

(a) Sintering atmosphere – Air/O_2
(b) Temperature
(c) Dwell time at temperature
(d) Original particle size
(e) Powder preparation route

3.1.1. Densification of powders

The powders prepared by calcining and grinding gave a sintering trace as shown in Fig. 1. The onset temperature of sintering was found to be affected by the initial particle size; the temperature being lower for smaller particle sizes. Also the lower the particle size the more complete was the densification. Perhaps of most importance was the sample preparation. Near full density (95–99%) was achieved in a number of the viscous processed samples. This allowed a good estimate of the theoretical Young's modulus to be made. Grain growth was found to be dependent on atmosphere, temperature and dwell time. This is dealt with in detail in the discussion of microstructure.

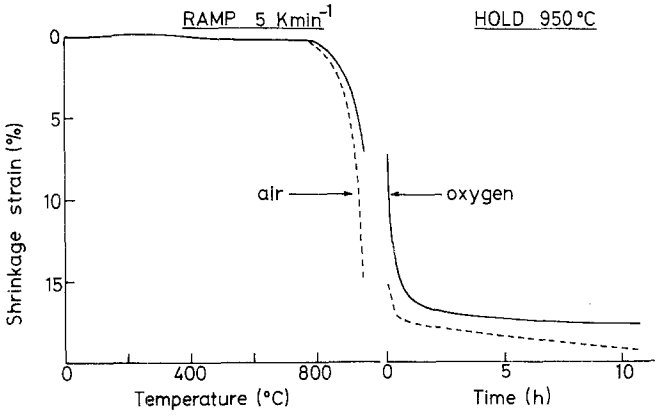

Figure 1 Densification of calcined powder.

The thermal expansion coefficient α varied according to atmosphere in the sintering furnace. For the air sintered material $\alpha = 14.7\,\mu m\,m^{-1}\,K^{-1}$ and for the O_2 sintered material $\alpha = 11.5\,\mu m\,m^{-1}\,K^{-1}$. (See Table I).

3.2. Microstructural examination

3.2.1. Optical microscopy

In a thin section in transmitted light the $YBa_2Cu_3O_{7-\delta}$ is opaque and has a very high refractive index suggestive of a high dielectric constant. In polished section examined in reflected light polysynthetic twinning is observed quite frequently. In an early sample where the green phase was present this was found to be pleochroic between almost colourless and blue-green. It is uniaxial negative, has no cleavage and a birefringence of approximately 0.025 (mid second order colours). The green phase occurred as elongate crystals with parallel extinction. The optical properties are consistent with trigonal, tetragonal or hexagonal compounds.

3.2.2. SEM

The sintering atmospheres strongly influenced the microstructure. This is shown in Figs 2 and 3. In Fig. 2 the air sintered sample has coarse grains, lath like in nature, some of which are in excess of 30 μm in length. The same material sintered in oxygen has a much finer more equiaxed granular microstructure.

The SEM micrograph shown in Figs 2 and 3 also show that air sintered materials appear to densify more easily for a given time and temperature in comparison with O_2 sintered samples. Fig. 4 shows that there is still considerable porosity after sintering under O_2 for 12 h at 925° C. Near theoretical density was achieved in calcined powders but only when these powders had been viscous processed and extruded to form rods. These samples are shown in Fig. 4a (as fired surface of rod) and Fig. 4b (fracture surface). Samples of the same powder which had been powder pressed and fired under the same conditions achieved 85–90% of theoretical density. In Figs 4a and b, it is seen that considerable grain growth has occurred. This becomes of crucial importance when flexural strength is discussed below.

Energy dispersive X-ray analysis on polished samples prepared by both powder pressing and viscous processing showed that the Y, Ba and Cu were dispersed very evenly throughout the polished surfaces. There was no area rich in any of these compounds. The resolution of the microprobe is such that it was not

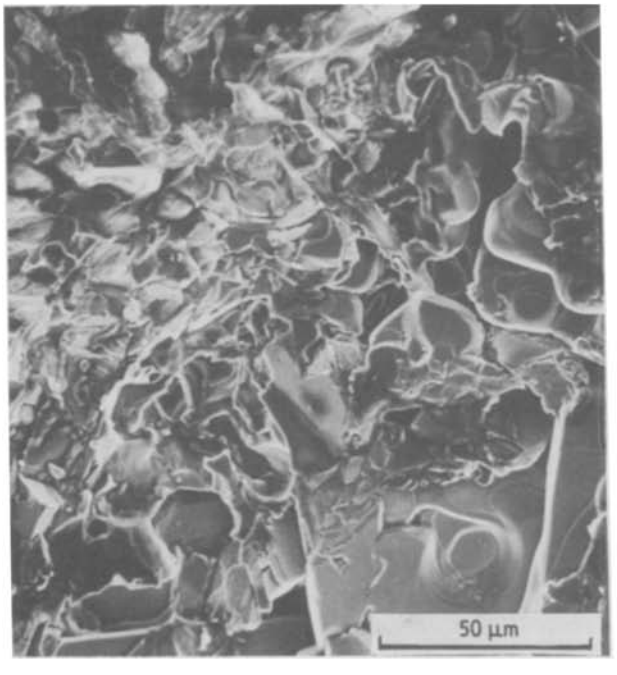

Figure 2 SEM of air sintered material.

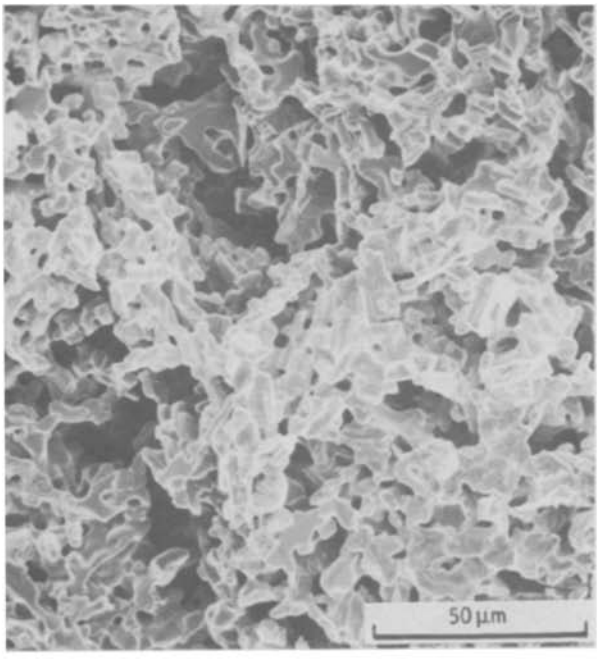

Figure 3 SEM of O_2 sintered material, 925° C 12 h.

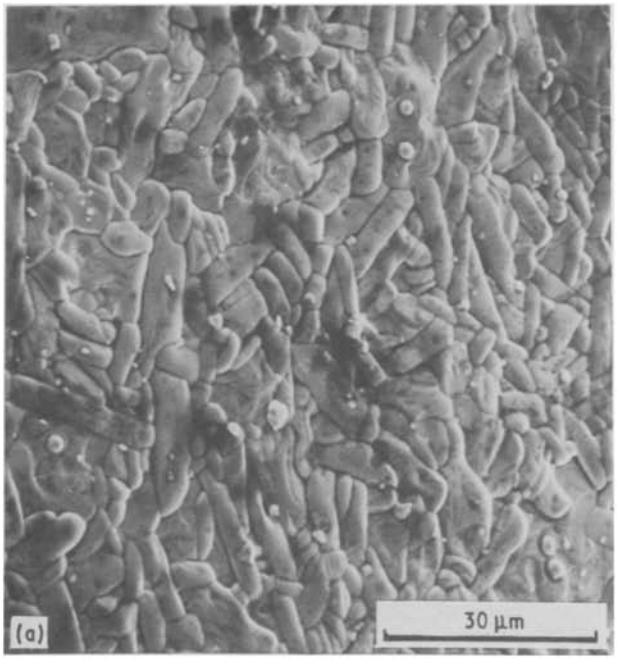

Figure 4a Near full density fired surface. (Sample $\varrho = \sim 0.98$TD) 890° C 10 h, 950° C 12 h, O_2.

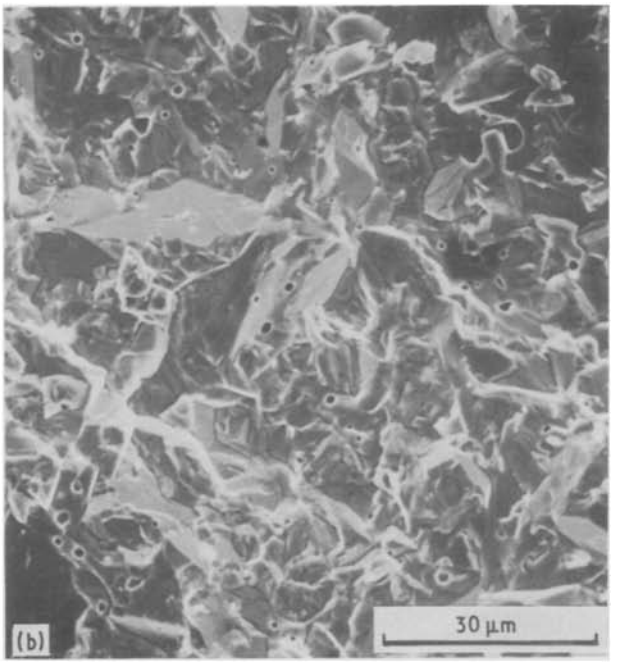

Figure 4b As Fig. 4a, fracture surface.

possible to tell if segregation had occurred on a fine scale, e.g. at the grain boundaries.

3.3. Mechanical properties

3.3.1. Young's modulus

Young's modulus was measured in bending on a series of viscous processed extruded rod samples which varied in density from near theoretical density to ~ 75% of theoretical density. The effect of porosity on Young's modulus is shown in Fig. 5. The theoretical curve has been drawn using Equation 5.

$$E = E_0 (1 - P)^3 \quad (5)$$

where E_0 is the Young's modulus at zero porosity and P is pore volume. Young's modulus of fully dense $YBa_2Cu_3O_{7-\delta}$ is calculated using Equation 5 to be 180 GPa. Caution must be employed in the measurement, however, for it was noted that some samples, although of relatively high density had abnormally low Young's modulus as shown in Fig. 5. These samples, although of relatively high density had abnormally low Young's modulus as shown in Fig. 5. These samples had many microcracks due to an unsatisfactory firing schedule or due to thermal expansion anisotropy which, although not contributing to the pore volume greatly, changed the compliance of the sample. It is quite possible to extrapolate to higher values of Young's modulus taking single point values for $E = 141$ GPa at a density of 86.8% of theoretical which then yields a value of $E = 214$ GPa by Equation 5.

3.3.2. Critical stress intensity factor, K_{IC}

K_{IC} was measured at room temperature (see Table I) and found to be ~ 1 MPa m$^{1/2}$. This means that the material is very brittle and cannot tolerate large defects. The fracture energy R was calculated from Equation 6.

$$R = K_{IC}^2/E \quad (6)$$

TABLE I Physical and mechanical properties of $YBa_2Cu_3O_{7-\delta}$

Surface area of powder ($m^2 g^{-1}$)	5.9	
Powder density ($g cm^{-3}$)	6.3	
Flexural strength, σ_f (MPa)	216.3 ± 16.4 (at 80.8% ϱ_{th})	
Young's modulus, E_b (GPa)	141.8 (at 86.8% ϱ_{th})	165 (at 97% ϱ_{th})
K_{IC} (MPa m$^{1/2}$)	1.07 ± 0.18 (at 80% ϱ_{th})	
Critical flaw size (μm)	14	
Fracture energy, R (Jm^{-2})	10	
Thermal expansion (50–450° C) Sintered and measured in air ($\mu m\, m^{-1} K^{-1}$)	14.6	
Thermal expansion (50–450° C) Sintered and measured in O_2 ($\mu m\, m^{-1} K^{-1}$)	11.5	
Specific heat at $\varrho = 4.52\, g cm^{-3}$ ($J kg K^{-1}$)	425	
Specific heat at $\varrho = 5.25\, g cm^{-3}$ ($J kg K^{-1}$)	431	
Thermal conductivity at $\varrho = 4.52\, g cm^{-3}$ ($W m^{-1} K^{-1}$)	1.55	
Thermal conductivity at $\varrho = 5.25\, g cm^{-3}$ ($W m^{-1} K^{-1}$)	2.67	

Note: At theoretical density if $E = 180$ GPa then $R = 5.5\, Jm^{-2}$. Both E_b and σ_f displayed some anomalously low values at near theoretical density due possibly to thermal expansion anisotropy.

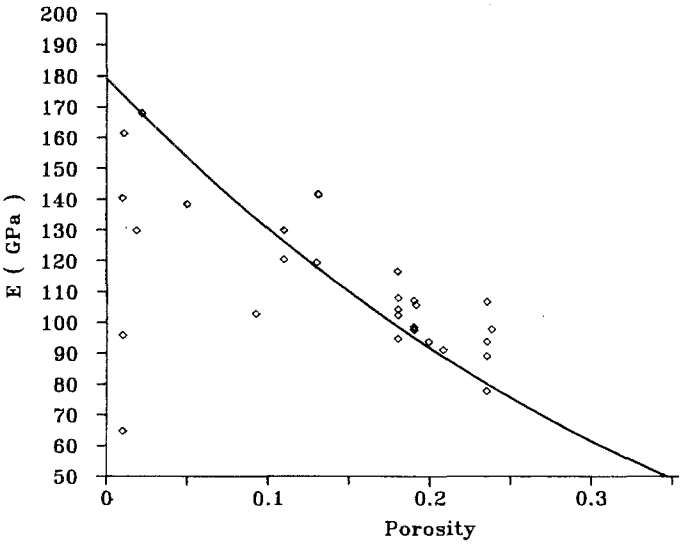

Figure 5 Young's modulus against porosity for $YBa_2Cu_3O_{7-\delta}$ (—) Equation 5, (◆) experimental.

This yields a value of fracture energy of $\sim 5.5\,Jm^{-2}$. This very low value for fracture energy poses serious limitations as to the manner in which these materials may be used. Clearly the defect size must be reduced to very small dimensions indeed to obtain strong materials, this is discussed in the next section. It should be noted that the samples which were used to measure K_{IC} contained $\sim 15\%$ porosity. The K_{IC} of fully dense material is expected to be somewhat higher than $1\,MPa\,m^{1/2}$.

3.3.3. Flexural strength

Flexural or tensile strength in brittle materials is governed by the Griffith [12] fracture criterion. In the $YBa_2Cu_3O_{7-\delta}$ materials the modulus and stress intensity factor have been measured yielding very low values for fracture energy ($5–6\,Jm^{-2}$). In order to increase strength, the flaw size estimated from Equation 1 must be reduced.

In the superconductor materials tested here we observed a spread in flexural strength from 80–250 MPa giving calculated flaw sizes in the range 100 to 10 μm (see Table I). Processing defects are clearly a problem in ceramics but the method we have developed gives exceptionally low defect sizes in other ceramics such as Al_2O_3 ($c = 10\,\mu m$) and TiO_2 ($c = 4.5\,\mu m$). The formation of large defects is believed to be related to the material itself and in all probability may be caused by the high thermal expansion coefficient ($\alpha = 11\,\mu m\,m^{-1}\,K^{-1}$). The achievement of high density which has been shown to be possible may cause problems on cooling whereas reaching a density of only 85% theoretical reduces the likelihood of cracking on cooling. (see the expression given in Equation 8).

Figure 6 Cracking thought to be caused by thermal effects. Note transgranular fracture.

$$\text{Thermal shock parameter} = \sigma_f/E\alpha \qquad (8)$$

Inserting values of $\sigma_f = 200\,MPa$, $E = 180\,GPa$ and $\alpha = 11 \times 10^{-6}$ yields a thermal shock parameter of 101° C. If the material is only 85% of theoretical density then the Young's modulus is $\sim 110\,GPa$ and this yields a thermal shock parameter of 165° C. This is still low when it is considered that Al_2O_3 with $\sigma_f = 500\,MPa$, $\alpha = 8 \times 10^{-6}$ and $E = 400\,GPa$ has a thermal shock factor of 156° C, and that Al_2O_3 is not noted for its thermal shock resistance. At present it is believed that there is thermal expansion anisotropy related to the crystallographic orientation [8]. Should this be the case then there may be a critical grain size above which thermal expansion anisotropy will cause cracking [13–15]. The dimensions of this critical grain size can only be deduced once the extent of the anisotropy is known. Using data given [8] we estimate the thermal expansion coefficient for the *a*, *b*, and *c* axes to be approximately $\alpha_a = 14.0\,\mu m\,m^{-1}\,K^{-1}$, $\alpha_b = 19.2\,\mu m\,m^{-1}\,K^{-1}$ and $\alpha_c = 19.4\,\mu m\,m^{-1}\,K^{-1}$. Equation 8 [15] gives the grain facet length L_c above which thermal stress will cause cracking

$$L_c = 3.1\,(K_b/(E\Delta\alpha\Delta T)) \qquad (9)$$

When K_b is the grain boundary fracture resistance, taken as $K_b = 1\,MPa\,m^{1/2}$, $E = 180\,GPa$, $\Delta\alpha = 5.4 \times 10^{-6}$ and $\Delta T = 900\,K$, L_c is then 4.05 μm, much smaller than the grain size we observed in fully dense materials. An example of cracking which may be due to thermal expansion anisotropy is shown in Fig. 6.

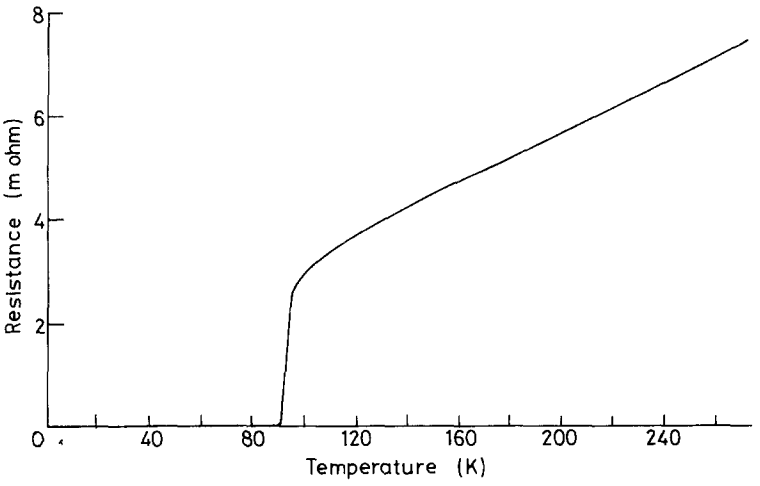

Figure 7 Resistance against temperature for $YBa_2Cu_3O_{7-\delta}$.

Note the trans-granular fracture. It is instructive to note that the samples which had the highest strengths were ~80–90% of theoretical density. At the highest densities we noted that there could be a considerable decrease in strength to ~50 MPa.

The limits to the strength of these materials depend on the considerations outlined above but using Equation 1 it can be seen that to reach strengths in excess of 500 MPa the critical defect size must be very low at ~2.5 μm (with K_{IC} = 1.0 MPa $m^{1/2}$). A summary of the physical and mechanical properties is given in Table I.

3.4. T_c, critical current

Fig. 7 shows a typical resistivity curve. The superconducting transition varied only slightly between samples. The transition width is ~1 K but some samples displayed a pronounced 'knee' 2 to 3 K below the temperature at which the resistivity dropped sharply. This may indicate the presence of more than one phase. The nearly linear high temperature resitivity data were found to have a negative intercept on the temperature axis when extrapolated to zero resistivity of ~ −100 K.

In the critical current experiment the voltage across the voltage leads rose slowly and continuously but at an increasing rate once the critical current was exceeded. Even for currents of twice the critical current V was far less than the normal value. Thus it appears that even though there is no longer a continuous superconducting path through the material, many superconducting regions remain. The highest critical current measured was just over 10^3 A cm^{-2}.

4. Comments on processing

As will be noted already we have both powder pressed samples and produced samples by a technique which we refer to as viscous processing. The limits to powder pressing are that only relatively simple objects are possible and of more importance we find that densification is hindered somewhat. The maximum density achieved in powder pressed samples was ~90–95% of theoretical density. Viscous processing enables quite complex shapes to be made by virtue of the fact that the green body with its polymer carrier is truly plastic. It is possible to make thin substrates (~100 μm in thickness) and of course much thicker plates as well as a variety of shapes by compression or injection moulding. Extrusion of rods, wires or pipes poses no problem whatever and we find that near theoretical density is achieved in 2 mm rods and rods or wires with smaller diameters. Examples of such forms are shown in Fig. 8.

5. Further work

This initial examination of the $YBa_2Cu_3O_{7-\delta}$ materials has highlighted a number of problems. First among these is the need for a suitable starting powder. The calcining route suffers from the problem of requiring a grinding stage and comminution of the powder to below a micron is a lengthy procedure which produces angular particles as an end product. Nevertheless, such powders did sinter to near theoretical density and gave samples with high strength (> 200 MPa in bending at 80–90% density).

The sintering behaviour of these materials is awkward in the sense that sintering takes place at temperatures close to the melting point (MP ≃ 1050° C). Densification is, therefore, a problem but densification is so strongly dependent on the starting powder characteristics that an improvement in the powder

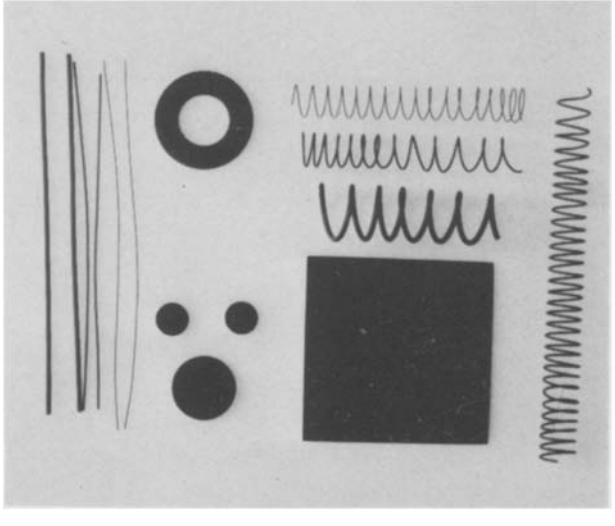

Figure 8 Extruded and moulded shapes of sintered $YBa_2Cu_3O_{7-\delta}$ material.

could well remove the problems associated with sintering. The critical current is at present low in these ceramic materials but improved microstructure is expected to raise the value. We measured critical currents of $\sim 800\,A\,cm^{-2}$ in porous (80% dense) materials. The critical current rose to $1000\,A\,cm^{-2}$ in material 90% of theoretical density. Reports of $100\,000\,A\,cm^{-2}$ [16] by Bell labs are in $1\,\mu m$ thick single crystal films where grain boundary and porosity effects are absent.

Use of these materials will also be dependent on whether processing techniques will produce strong materials. In our experience powder pressing generally gives poor strength in comparison with viscous processed bodies. Also it is noted that only viscous processed materials densified to near theoretical density. Only small flaws can be tolerated because of the low K_{IC}, $K_{IC} = 1\,MPa\,m^{1/2}$. This low value places even more emphasis on improved processing. A key problem which must be addressed is that associated with what is believed to be thermal stresses which cause cracking. As noted earlier some of the samples which attained high density (~ 0.98 of ϱ_{th}) displayed anomalously low strength and Young's modulus. This could be explained by the presence of fine microcracks (shown in Fig. 6) which do not alter the density significantly but which would have a deleterious effect on the strength (through Equation 1) and which would change the compliance of the sample thereby lowering the Young's modulus.

Full density did not always give improvements in strength and modulus. As noted in the text and in Fig. 5 the Young's modulus decreased due possibly to the presence of microcracking. The maximum value for Young's modulus was 165 GPa at $\sim 97\%$ of theoretical density. The flexural strength at high density (97% of TD) was ~ 100 MPa but cracking due possibly to thermal expansion anisotropy reduced strength to values of 30 to 60 MPa. The value of 100 MPa may also be low due to cracking.

6. Conclusions

The physical and mechanical properties of $YBa_2Cu_3O_{7-\delta}$ superconducting ceramics have been investigated. The powder was prepared by calcining mixed oxides and grinding to yield a powder with a surface area of $5.9\,m^2\,g^{-1}$.

These materials were either powder pressed or viscous processed, the latter being favoured. It was found that significant differences existed between air and oxygen atmospheres during firing. Those differences manifested themselves in degree of grain growth and densification. Near fully dense materials could be obtained only on viscous processed samples. In the near fully dense materials Young's modulus was measured to be 165 GPa from which it was estimated that the Young's modulus of dense material was 180 GPa. The strength in bending was found to be 216 MPa for the extruded material made from calcined powders. K_{IC} on material $\sim 80\%$ of full density was found to be $K_{IC} = 1.07\,MPa\,m^{1/2}$.

This paper has shown that the microstructural development is determined by starting powder, sintering schedule and atmosphere. The mechanical properties are determined by the microstructure and we have shown that because the fracture toughness of the material is low, the need is therefore to develop methods of processing which eliminate processing flaws. Viscous processing is one method which reduces processing flaws to small dimensions ($\sim 15\,\mu m$ in the $YBa_2Cu_3O_{7-\delta}$) allowing bend strength in the material of ~ 200 MPa to be achieved. We have noted that thermal stresses may be a problem leading to anomalously low values of Young's modulus and strength due to microcracks.

The problem of thermal expansion anisotropy has been examined and using data from reference [8] we calculate that the maximum grain facet length should be $\sim 4\,\mu m$. Sintering the materials to near full density was associated with grain growth in excess of $4\,\mu m$. This examination of $YBa_2Cu_3O_{7-\delta}$ as a ceramic material suggests that if high mechanical properties are required, considerable attention must be paid to reducing the sintering temperature. This would avoid problems such as microcracking caused by thermal expansion anisotropy by reducing grain growth and allow the preservation of the optimum oxygen content.

Acknowledgements

Thanks are due to Dr Robert Hall, University College London, for optical microscopy examination and to Geoff Dolman and John Whitehouse for assistance with experimental work. The thermal diffusivity and thermal conductivity measurements were performed by Dr Steve Preston at UKAEA, Springfields.

References

1. J. G. BEDNORZ and K. A. MULLER, *Z. Phys.* **B64** (1986) 189.
2. C. W. CHU, D. H. HOR, R. L. MENG, L. GAO, Z. J. HUANG and Y. Z. WANG, *Phys. Rev. Lett.* **58** (1987) 405.
3. M. K. WU, J. R. ASHBURN, C. J. TORNG, P. H. HOR, R. L. MENG, L. GAO, Z. J. HUANG, Y. Q. WANG and C. W. CHU, *Phys. Rev. Lett.* **58** (1987) 908.
4. E. M. ENGLER, V. Y. LEE, A. I. NAZZAL, R. B. BEYERS, G. LIM, P. M. GRANT, S. S. P. PARKIN, M. L. RAMIREZ, J. E. VAZQUEZ and R. J. SAVOY, *J. Amer. Chem. Soc.* **109** (1987) 2848.
5. W. I. F. DAVID, W. T. A. HARRISON, J. M. F. GUNN, O. MOZE, A. K. SOPER, P. DAY, J. D. JORGENSEN, D. G. HINKS, M. A. BENO, L. SODERHOLM, D. W. CAPONE, I. K. SCHULLER, C. U. SEGRE, K. ZHANG and J. D. GRACE, *Nature* **237** (May 1987) 310.
6. D. J. EAGLESHAM, C. J. HUMPHREY, W. J. CLEGG, M. A. HARMER, N. McN. ALFORD and J. D. BIRCHALL, "Advanced Ceramic Materials", Vol. 2, No. 3B (1987) p. 662.
7. D. J. EAGLESHAM, C. J. HUMPHREY, N. McN. ALFORD, W. J. CLEGG, M. A. HARMER and J. D. BIRCHALL, *Appl. Phys. Lett.* **51** (1987) 457.
8. P. K. GALLAGER, H. M. O'BRYAN, S. A. SUNSHINE and D. W. MURPHEY, *Mat. Res. Bull.* **22** (1987) 995.
9. P. STROBEL, J. J. CAPPONI, C. CHAILLOUT, M. MAREZIO and J. L. THOLENCE, *Nature* **327** (May 1987) 306.
10. N. McN. ALFORD, J. D. BIRCHALL, A. J. HOWARD, K. KENDALL and J. H. RAISTRICK, European Patent publication No. 183453 (1986).
11. W. F. BROWN and J. E. SRAWLEY, Plane strain crack

toughness testing of high strength metallic materials. ASTM STP 410 (American Society for Testing and Materials, Philadelphia, Pennsylvania, 1966).
12. A. A. GRIFFITH, *Phil. Trans. R. Soc. London Series A* **221** (1920) 163.
13. A. G. EVANS, *Acta Metall* **26** (1978) 1845.
14. R. W. RICE, R. C. POHANKA and W. J. McDONOUGH, *J. Amer. Ceram. Soc.* **63** (1980) 703.
15. A. G. EVANS and Y. FU, in "Advances in Ceramics", Vol. 10, edited by W. D. Kingery (American Ceramic Society, Columbus, Ohio, 1984) 697.
16. *High Tech Materials Alert* **4**, No. 6 (1987) 3.

Received 5 August
and accepted 25 August 1987